Controlling the Capture and Release of DNA with a Dual-Responsive Cationic Surfactant

Lu Xu, Lei Feng, Jingcheng Hao, and Shuli Dong*

Key Laboratory of Colloid and Interface Chemistry & Key Laboratory of Special Aggregated Materials, Shandong University, Ministry of Education, Jinan 250100, China

Ⓢ *Supporting Information*

ABSTRACT: A dual-responsive cationic surfactant, 4-ethoxy-4′-(trimethyl- aminoethoxy) azobenzene trichloromonobromoferrate (azoTAFe), which contains both a light-responsive moiety azobenzene and a paramagnetic counterion, $[FeCl_3Br]^-$, was designed and synthesized. Not only does this cationic surfactant abundantly utilize inexhaustible and clean sources, i.e., light and magnetic field, but it also serves as a powerful dual-switch molecule for effectively controlling the capture and release of DNA. Our results could provide potential applications in gene therapy for creating smart and versatile machines to control the transport and delivery of DNA more intelligently and robustly. It was proved that the light switch can independently realize a reversible DNA compaction. The introduction of a magnetic switch can significantly enhance the compaction efficiency, help compact DNA with a lower dosage and achieve a magnetic field-based targeted transport of DNA. In addition, the light switch can make up the irreversibility of magnetic switch. This kind of self-complementation makes the cationic azoTAFe be useful as a potential tool that can be applied to the field of gene therapy and nanomedicine.

KEYWORDS: DNA, capture and release, dual-switch, light and magnet, cationic surfactant
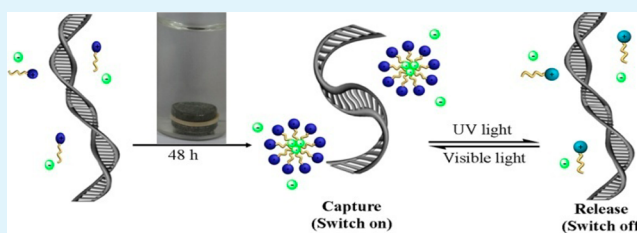
1. INTRODUCTION

Gene therapy, which can be realized by transporting functional DNA fragments to target cells for helping the repair of the disabled gene to function well, is of great importance in curing genetic diseases and cancer, and culturing specific functional cells, etc.[1−4] Because of electrostatic or conformational reasons, DNA cannot cross cell membranes independently.[5,6] Thus, one of the major challenges in gene therapy is to find proper tools or vectors for effectively transporting functional DNA fragments to target cells and achieve an efficient gene delivery in cells.

Cationic surfactants have been used with some success for transporting and compacting DNA. The binding of cationic micelles on DNA backbones can reduce the charge repulsion between adjacent phosphate groups, and make them approach each other, leading to the so-called "compaction" of DNA.[7,8] The reduction both in the size of DNA molecules and the repulsion with phospholipid bilayers produce more opportunities for them to cross cell membranes.[9−11] The critical micelle concentration (cmc) of a cationic surfactant in the presence of DNA (often defined as critical association concentration (cac)[12]) is normally much lower than that in aqueous solution in the absence of DNA.[12] Under controlling conditions such as formation of cationic and anionic (catanionic) surfactant micelles,[12] adding β-CD,[13] or salts,[14] the binding of cationic micelles can be disrupted, the captured DNA will be released, and the aim of gene delivery can be realized.[12−14]

Although DNA/surfactant mixtures show potential applications in regulation of the DNA delivery, with the growth of gene therapy technology, there still exists challenges in further development of multifunctional machines with high sensitivity, remote controllability, and external actuated properties that can be applied more intelligently and more powerfully to control both the transport and suppression of DNA. To solve such problems, we designed and synthesized a dual-responsive cationic surfactant, azoTAFe (the synthesis pathway was illustrated in Scheme 1, which was presented in Supporting Information). The cationic azoTAFe contains both a light-responsive azobenzene group[15,16] as well as a paramagnetic counterion, $[FeCl_3Br]^-$.[17,18] The inherent characteristic trans-to-cis isotherm interconversion of the azo-group upon alternately being exposed to UV and visible light[15,16] can be used to control the formation of azoTAFe micelles, thereby enabling it to act as one kind of molecular switch for effectively regulating the capture and compaction of DNA via adjusting light sources. The paramagnetic $[FeCl_3Br]^-$ ion can successfully serve as a magnetic-switch to allow the surfactants to reach an effective concentration around magnetic fields,[17,18] making this kind of surfactant be able to compact DNA with a lower dosage and enhance the compaction efficiency in the presence of an external magnetic field. The conjunction of DNA and azoTAFe

Scheme 1. Synthesis Route of azoTAFe
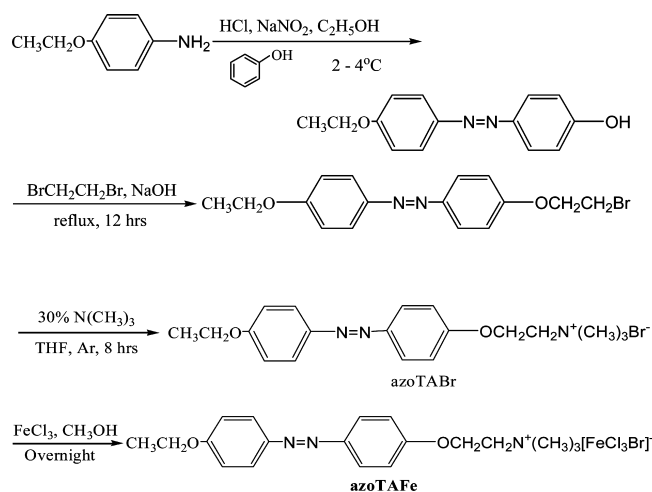
results in ferromagnetic aggregates, which are able to be controlled by magnetic force[19,20] and provide an effective magnetic field-based DNA targeted transport. Having self-complementation, the light switch can make up the irreversibility of the magnetic-triggered transport and capture of DNA. This could make azoTAFe provide an unprecedented strategy of dual-switchable capture and release of DNA, which is envisioned to find potential applications in gene therapy and biotechnology.

2. EXPERIMENTAL SECTION

Chemicals and Materials. Herring testes double-strand DNA sodium salts were purchased from Sigma. Its molar weight was <1200 bps determined by agarose gel electrophoresis (AGE) and its concentration was examined through considering the DNA bases molar extinction coefficient to be 6600 mol^{-1} cm^{-1} at 260 nm. The absorbance ratio of DNA stock solution was 1.8 to 1.9 at 260 and 280 nm, which suggests no protein was present.

azoTAFe was prepared by mixing equal molar amounts of iron trichloride (FeCl$_3$) with synthetic 4-ethoxy-4′-(trimethylaminoethoxy) azobenzene bromide (azoTABr) in methanol and stirring overnight at room temperature.[17,18] The solvent was then removed and the product was dried at 80 °C overnight yielding brown/red solids. The critical micelle concentration (cmc) as well as the dissociation constant of azoTAFe was determined by electrical conductivity method to be about 0.6 mmol L^{-1} and 0.66, respectively (Figure S1b in the Supporting Information). SQUID magnetometry (Figure S1a in the Supporting Information) showed that this compound is a completely paramagnetic substance at room temperature. FeCl$_3$ was purchased from Sinopharm Chemical Reagent Co. Ltd., China.

Analytical TLC was performed on Merck silica gel 60 F254 plates and all compounds were visualized by UV light. Column chromatography was carried out by using silica gel 60 (200−300 mesh). ^{1}H NMR spectroscopic measurements were carried out by using a Bruker Avance 400 MHz NMR spectrometer, and chemical shifts were referenced to internal standards TMS (δ = 0.00 ppm). High-resolution mass spectrometry (HR-MS) was performed using a MicroTof spectrometer (Agilent).

Sample Preparation. dsDNA stock solutions were prepared in 10 mmol L^{-1} tris-HCl buffer (pH = 7.4). All the samples at constant concentration of DNA (0.075 mmol L^{-1}) with an increase of azoTAFe were prepared by mixing known amounts of DNA, cationic surfactant and water to a fixed final volume (3 mL) in plastic centrifuge tubes. All samples were left for 24 h at 25 °C for equilibration, then proper centrifugation at 8000 rpm for 10 min was used to remove precipitates before conducting each measurement. Thrice-distilled water was used to prepare all the sample solutions.

Electrical Conductivity. A DDSJ-308A analyzer was used to perform electrical conductivity experiments. A Pyrex glass measuring cell was placed in a water bath at 25.0 ± 0.3 °C. The cmc was determined from the break point between the higher $[d\kappa/d(conc)]$ and lower $[d\kappa/d(conc)]$ linear curves. The surfactant ionic dissociation constant (β) was estimated by the ratio of the two slopes.

SQUID Magnetometry. Dried samples of surfactant or DNA/surfactant complexes were placed in sealed polypropylene tubes and mounted inside a plastic straw for measuring in a magnetometer with a superconducting quantum interference device (MPMSXL, Quantum Design, USA) and a reciprocating sample option (RSO). The data were collected at 300 K.

Irradiation Experiments. A CHF-XM35−500W ultra high-pressure short arc mercury lamp equipped with two light sources was utilized for light irradiation experiments to isomerize azobenzene moieties from trans- to cis-state in UV light (350 nm) and cis- to trans-state in visible light (455 nm).

UV−Visible Spectrometry. UV spectra of DNA/surfactant complex solutions were examined by a U-4100 UV−visible spectrometer, using a 10 mm path length quartz cell at a wavelength range of 220−320 nm. When the samples were measured for UV−visible spectra, proper background subtraction was conducted for the samples with precipitates by water or without precipitates by equal amount surfactant solution as references.

Circular Dichroism (CD). A JASCO J-810 spectropolarimeter was used to perform CD spectra. Samples were located in 10 mm path length cells, and the scanning speed was controlled to be 100 nm min^{-1} with the measuring range from 220 to 320 nm. Each sample was measured three times for the average value. The number of repeats of each sample was set to be 3, the resulting average curves were calculated automatically.

Dynamic Light Scattering (DLS). A BI-200SM instrument (Brookhaven) was used for the measurements of DNA/surfactant complex solution samples at a constant scattering angle of 90°. All solutions were made dust-free by filtration through cellulose acetate membranes of 0.45 mm pore size. DLS data were measured the correlation functions ten times and reported the average of the 10 CONTIN analyzes.

Agarose Gel Electrophoresis (AGE). Agarose gels (1% w/vol) were horizontally submerged in pH 7.4 TAE buffer (40 mmol L^{-1} Tris, 2 mmol L^{-1} Na$_2$EDTA·2H$_2$O, 20 mmol L^{-1} glacial acetic acid) at 5 V/cm. DNA was visualized by ethidium bromide (0.5 μg mL^{-1}), and a standard DNA ladder of 5000 bps was utilized as a reference. This measurement was conducted in a darkroom with aluminum foil packing around the electrophoresis tank.

Atomic Force Microscopy (AFM). A Nanoscope IIIA (veeco) was used to capture DNA/surfactant complexes formed at different cases. A drop of 1 μL sample solution was deposited on a clean mica plate and lyophilized for 12 h (−65 °C, 0.05 mbar) before being measured. Etched silicon probes with a nominal spring constant of 40 N m^{-1} (Digital Instruments, model RTESP7) were used. All images were recorded with a tapping mode at 512 × 512 pixel resolution and a scan speed of 1.0 Hz. Each image was analyzed with the Nanoscope software (version 5.30r3sr3).

3. RESULTS AND DISCUSSION

Multivalent species with at least three positive charges are required to compact DNA.[21] Cationic surfactants can compact DNA lies on that they self-assemble into micelles in the vicinity of DNA.[9] The binding of cationic micelles can not only effectively reduce the charge repulsion but also induce effective attraction among different parts of the DNA chain to favor the compaction of DNA.[7,8] To probe potentials of the azoTAFe in transporting and compacting DNA, we performed the measurements of UV−vis, CD, and DLS to obtain a basic understanding on the interaction behavior of DNA with different amounts of azoTAFe. A range of concentrations where azoTAFe can self-assemble into micelles in the vicinity of
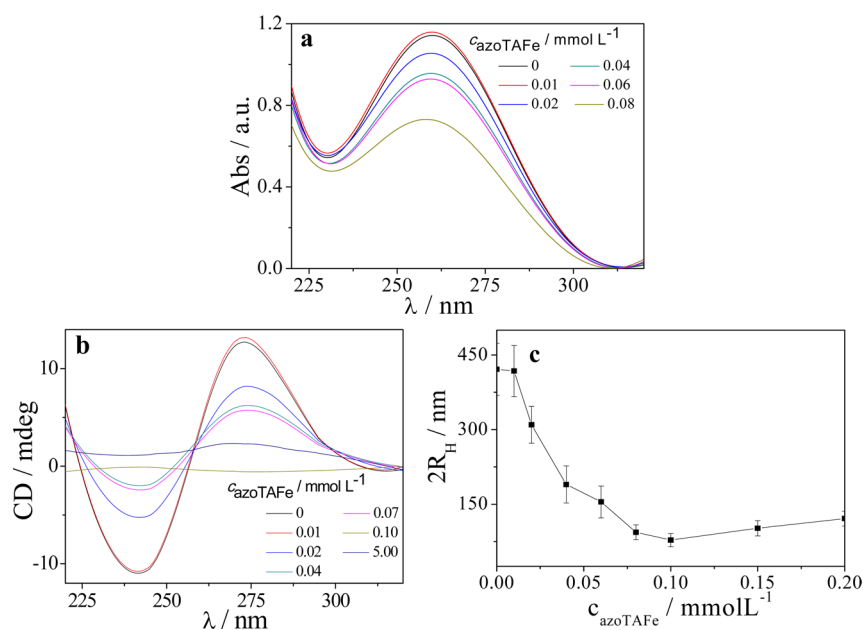
Figure 1. (a) UV spectra, (b) CD spectra, and (c) the average hydrodynamic diameters of a $c_{DNA} = 0.075$ mmol L^{-1} with different amounts of azoTAFe. $T = 25.0 \pm 0.1$ °C.

DNA for capturing and compacting DNA with the maximum efficiency were determined.

Reduction in optical density at $\lambda_{max} = 260$ nm (OD$_{260}$) of 0.075 mmol L^{-1}DNA in UV–vis spectra (Figure 1a) showed that the compaction started at $c_{azoTAFe} = 0.02$ mmol L^{-1},[11] meaning that the lowest concentration for efficient DNA capture is 0.02 mmol L^{-1} azoTAFe. The CD spectra revealed that DNA possesses a positive band at 275 nm of the base stacking and a negative band at 242 nm of the helicity (Figure 1b).[22] At $c_{azoTAFe} = 0.02$ mmol L^{-1}, the intensity decreased and the red shift of the two main bands was discovered, indicating that the appearance of DNA condensation,[22] and the critical concentration was in accord with the UV data. DLS (Figure 1c) data showed that the decrease of R_H also started at $c_{azoTAFe} = 0.02$ mmol L^{-1}, and the maximum reduction of DNA size was above 82.5% at $c_{azoTAFe} = 0.10$ mmol L^{-1}.

The azoTAFe has been demonstrated as a good compaction agent; the remaining problem is how to control the release and decompaction of DNA for achieving delivery in vitro. Under visible light, azobenzene-based cationic surfactants can exist as a hydrophobic trans-state.[15,16] After azoTAFe is exposed to UV irradiation, it can convert to a relatively hydrophilic cis-state.[15,16] The hydrophilicity of azo-surfactants increases after illuminated by UV light, resulting in the increase of cac of azoTAFe.[15] As a result, the azobenzene moiety of azoTAFe can act as a powerful molecular switch for regulating a reversible DNA capture and compaction via converting the light irradiation. Once DNA was compacted, the binding of cationic micelles can obviously reduce the charge repulsion between adjacent DNA backbones. As a result, if DNA concentration is sufficiently high, the mixtures of DNA and cationic surfactants can aggregate and precipitate from solutions.[9] Therefore, the phase separation also acts as an indication of the compaction. The phase diagram of DNA mixed with trans- or cis-azoTAFe is shown in Figure 2a, in which the conformational changes of DNA triggered by UV and visible light can be traced by the phase separation.[9] The phase separation of the DNA/trans-azoTAFe mixtures occurs at $c_{azoTAFe} = 0.02$ mmol L^{-1}. It is in

accord with the UV, CD, and DLS data (Figure 1a–c). The phase separation phenomenon requires 0.07 mmol L^{-1} cis-azoTAFe for the DNA/cis-azoTAFe system. It suggests that the cac of azoTAFe with the trans-state is much lower than that with the cis-state. The amount of azoTAFe in the range of 0.02 < $c_{azoTAFe}$ < 0.07 mmol L^{-1} can be used to realize a reversible capture and compaction of DNA by converting the light source. Figure 1c shows that within the desired concentration range the sample of 0.06 mmol L^{-1} azoTAFe has the best compaction efficiency with a maximum size reduction of 69%, which was selected as a model sample to study the light switchable capture and release of DNA. After the sample was irradiated by UV light for 15 min, the originally variation of OD$_{260}$ in the UV spectra, both the positive and the negative bands in the CD spectra, and the size distribution in DLS intensity of DNA caused by the compaction were converted to that of pure DNA in aqueous solution (Figure 2b–d), indicating the existence of DNA release and decompaction behavior.[12−14] The transition kinetics between the compaction and decompaction state of 0.075 mmol L^{-1} DNA mixed with 0.06 mmol L^{-1} azoTAFe under different light irradiation were performed in Figure 2e, in which the concrete changes of OD$_{260}$ vs. irradiation time of UV and visible light, respectively, clearly suggest that both the conformational transition of DNA from compaction state to decompaction state in UV light and from decompaction state to compaction state under visible irradiation can be rapidly completed within 5 min. Light-switching stability was also verified by variations in OD$_{260}$ in the UV spectra as well as average hydrodynamic diameters of DNA by DLS data with the same sample of 0.075 mmol L^{-1} DNA/0.06 mmol L^{-1} azoTAFe illuminated by visible and UV light alternately for 15 min (Figure 2e, f). The OD$_{260}$ values drastically turned into 0.963 under UV irradiation and almost completely recovered when the sample was exposed to visible light. This light-induced change of OD$_{260}$ was completely reversible. It could be repeated for at least three cycles without any degradation. The hydrodynamic diameters gave out similar variation after the sample was alternately exposed to UV and visible light. These
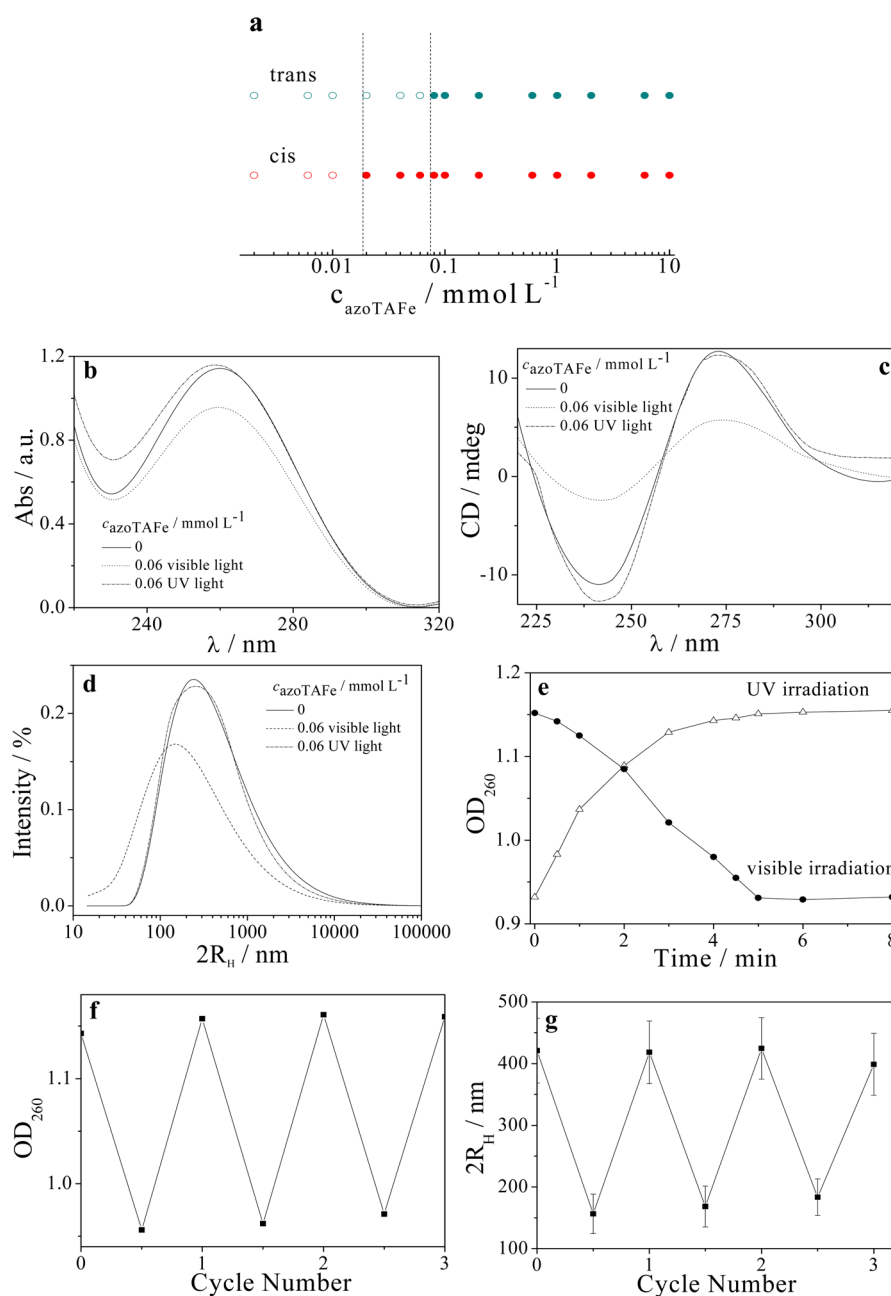
Figure 2. (a) Phase diagram of 0.075 mmol L^{-1} DNA mixed with trans-azoTAFe under visible light or *cis*-azoTAFe after UV irradiation, the filled symbols refer to the regions where precipitates can form. (b) UV spectra of pure DNA and DNA/0.06 mmol L^{-1} azoTAFe sample with visible or UV light, respectively. (c) CD data of light-switchable condensation of 0.075 mmol L^{-1} DNA/0.06 mmol L^{-1} sample regulated with different light sources. (d) DLS intensities of the 0.075 mmol L^{-1} DNA/0.06 mmol L^{-1} azoTAFe sample after irradiated by different light sources. (e) Variation in OD$_{260}$ showing the DNA progressively released from azoTAFe micelles under UV irradiation as well as the DNA progressively captured by azoTAFe micelles under visible irradiation. (f) Variation in OD$_{260}$ of 0.075 mmol L^{-1} DNA/0.06 mmol L^{-1} azoTAFe sample exposed to different light sources. (g) Change in average hydrodynamic diameters of 0.075 mmol L^{-1} DNA/0.06 mmol L^{-1} sample were irradiated by different light sources. T = 25.0 ± 0.1 °C.

results clearly show that the light-reversible capture and release of DNA exhibit a good reproducibility and a good reversibility.

SQUID magnetometry revealed that cationic azoTAFe is a typical paramagnetic surfactant (Figure S1a in the Supporting Information). This kind of surfactant can not only be magnetized but also be attracted by external magnetic fields.[19,20] We supposed that azoTAFe molecule exhibits a strong tendency to migrate toward an applied magnetic field and leads to a concentration enrichment in its vicinity. To demonstrate the concentration enrichment behavior in a

magnetic field and further explore potentials in compacting DNA with a lower dosage, we introduced an external magnet to concentrate a surfactant solution with a lower concentration, i.e., <0.02 mmol L^{-1}. The experiment started with a weak NdFeB magnet (0.25 T) placed in the bottom of a solution containing 0.01 mmol L^{-1} azoTAFe or complexes of 0.075 mmol L^{-1} DNA/0.01 mmol L^{-1} azoTAFe (the method is shown in Figure 3a), respectively. After 24 h, for azoTAFe system, the bottom solution was taken out and measured by the UV−vis spectra. As presented in Figure 3b, a significant
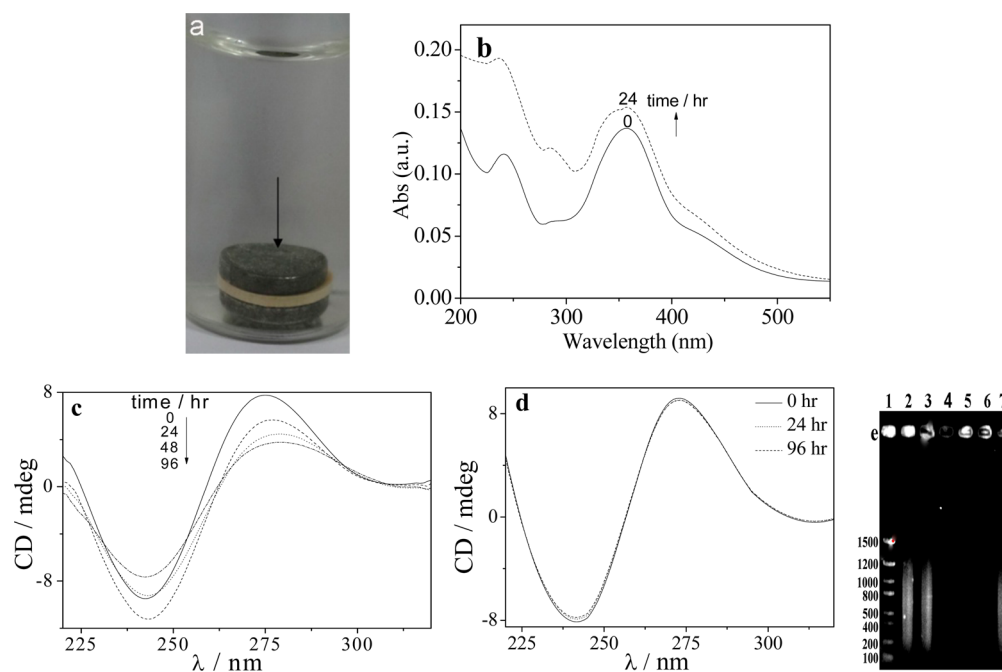
Figure 3. (a) Photograph using a magnet to induce the DNA compaction at a lower dosage of azoTAFe, the arrow refers to DNA/surfactant precipitates attached on the NdFeB magnet. (b) UV evidence of the concentration enrichment of 0.01 mmol L^{-1} azoTAFe induced by an external magnetic field after 24 h. (c) CD evidence of the DNA compaction induced by 0.01 mmol L^{-1} azoTAFe in the presence of an external magnet (0.25 T) at different times (d) with the same sample in the absence of a magnetic field as a reference. (e) AGE results of the time-dependent compaction of DNA induced by a magnet: lane 1 refers to a DNA molecular weight marker, the labeled number refers to the molecular weight (bps) of the reference DNA on the marker, lane 2 refers to the sample containing free DNA and lane 3 is the mixture of 0.075 mmol L^{-1} DNA/0.01 mmol L^{-1}. Samples after the introduction of a magnet for 24, 48, 96 h are collected in lanes 4, 5, and 6 respectively. Lane 7 is the sample of lane 5 exposed to UV light.
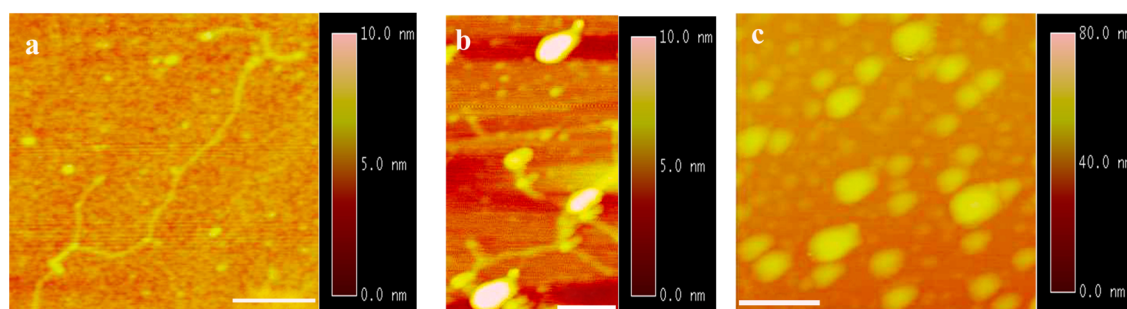

Figure 4. (a) AFM images of DNA/trans-azoTAFe complexes formed in different cases, stretched DNA coexisting with 0.01 mmol L^{-1} azoTAFe micelles without a magnet. (b) Coexisting coil-globular state of DNA with 0.01 mmol L^{-1} azoTAFe after the introduction of a magnet (0.25 T) for about 24 h. (c) Completely globular compacted DNA with 0.01 mmol L^{-1} azoTAFe after being in a magnetic field for 48 h. Each labeled length scale bar is equal to 100 nm and the height scale bars were shown.

increase in the two main absorbance bands of azoTAFe at 355 and 240 nm can be traced. It indicates that azoTAFe molecules reach an effective concentration around the magnet, and thereby confirming the ability of a magnetic field in enhancing locally the concentration of azoTAFe. The migration behavior toward external magnetic fields was expanded to help compact DNA with a lower dosage. In a 0.075 mmol L^{-1} DNA/0.01 mmol L^{-1} azoTAFe complex system, after introducing a magnet for 24 h, a clear variation in the two main bands of the CD spectra demonstrated the DNA compaction (Figure 3c). It can be seen that the spectra exhibit continuous changes vs. time. However, in the absence of a magnetic field, no variation in DNA bands can be found over 96 h (Figure 3d), indicating that no compaction occurred. This gradual compaction process of DNA vs. time promoted by a magnet was also demonstrated

by agarose gel electrophoresis (AGE). In an AGE, the disappearance of the fluorescent signal of DNA in lanes 4−6 (Figure 3e) can be observed with the fluorescent dye ethidium bromide (EB) excluded from the double helix because of the binding of cationic micelles.[23,24]

Atomic force microscopy (AFM) offers direct observations of the magnetic induced DNA compaction. DNA molecules in the stretched state in a 0.01 mmol L^{-1} azoTAFe solution without a magnet are clearly displayed in Figure 4a. After a magnet was introduced for 24 h, condensed globular DNA along with uncompacted DNA of the stretched state coexisted (Figure 4b and Figure S2a in the Supporting Information), indicating that the capture of DNA had begun. After 48 h in the magnetic field, DNA was completely compacted and only the globular state

was observed (Figure 4c and Figure S2b in the Supporting Information).

As shown in Figure 5, DLS data clearly show that the DNA compaction efficiency can be regulated by 0.01 mmol L^{-1}
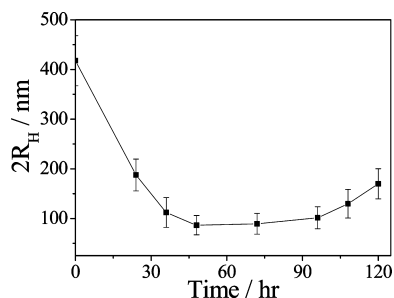

Figure 5. Progressive DNA compaction caused by a magnet (0.25 T) proved by DLS measurements. $T = 25.0 \pm 0.1$ °C.

azoTAFe in the presence of a magnetic field. The compaction efficiency reached a maximum at 48 h with a final size reduction of 80%. It was much higher than that of the sample with high amount of surfactant, e.g., 0.06 mmol L^{-1} azoTAFe with a 69% size reduction. This enhancement in compaction efficiency may be brought by the increase in the local concentration of surfactant in the vicinity of the magnet, which facilitates the formation of azoTAFe micelles. AFM and DLS measurements clearly predicate that the introduction of a magnetic switch can offer much better compaction efficiency with a lower dosage.

Dobson et al. reported that DNA molecules are diamagnetic, there always requires addition of magnetic nanoparticles to bind to DNA in order to control the migration as well as the targeted delivery of DNA in the presence of external magnetic force.[25] Interestingly, the combination of DNA and cationic azoTAFe micelles resulted in the formation of ferromagnetic aggregates with a typical "hysteresis loop" shown in Figure 6a.

The effective magnetic moment was measured to be 0.098 emu g^{-1}. That is the binding with azoTAFe micelles can make diamagnetic DNA molecules turn ferromagnetic and controlled by external magnetic force, and the magnetism implies potentials in realizing the targeted transport.[19,20] The reason why azoTAFe micelles can magnetize DNA could be explained by classical models describing colloid particles[26−29] as well as the work published by Eastoe et al.[17,18] According to classical models,[26,27] electric double layer of colloid particles are divided into two regions, the so-called Stern and diffuse layers. In the Stern layer, counterions are strongly bound and move with the particles as a whole dynamic entity. In the second, counterions move freely in the bulk and maintain dynamic equilibrium with those in the Stern layer. The surface that separates the two layers is a slipping plane. The location of the slipping plane is quite sensitive to the presence of polyelectrolytes, and the interaction with oppositely charged polyelectrolytes normally causes a displacement in the two layers and leads to the release of counterions in the diffuse layer.[26−29] Therefore, as azoTAFe micelles binds on DNA backbones, the magnetic $[FeCl_3Br]^-$ ions in the diffuse layer will be released by the charge competition, but those in the Stern layer remain unchanged and can magnetize DNA with micelles binding on it. Moreover, according to the work of Eastoe et al.,[17,18] not only the $[FeCl_3Br]^-$ counterions but also all the magnetic f-block coordination counterions, i.e., $[CeCl_3Br]^-$, $[GdCl_3Br]^-$, $[HoCl_3Br]^-$, are hydrophobic and present strong hydrophobic interaction with the alkyl chains of cationic surfactants. This specificity of these magnetic counterions make them able to partition into the core of cationic micelles because of the hydrophobic interaction with the alkyl chains.[17,18] With micelles combining with DNA, the magnetic $[FeCl_3Br]^-$ ions in the core of azoTAFe micelles also contribute to the magnetization of DNA. In summary, the ability of azoTAFe in magnetizing DNA can be attributed to a interplay between the
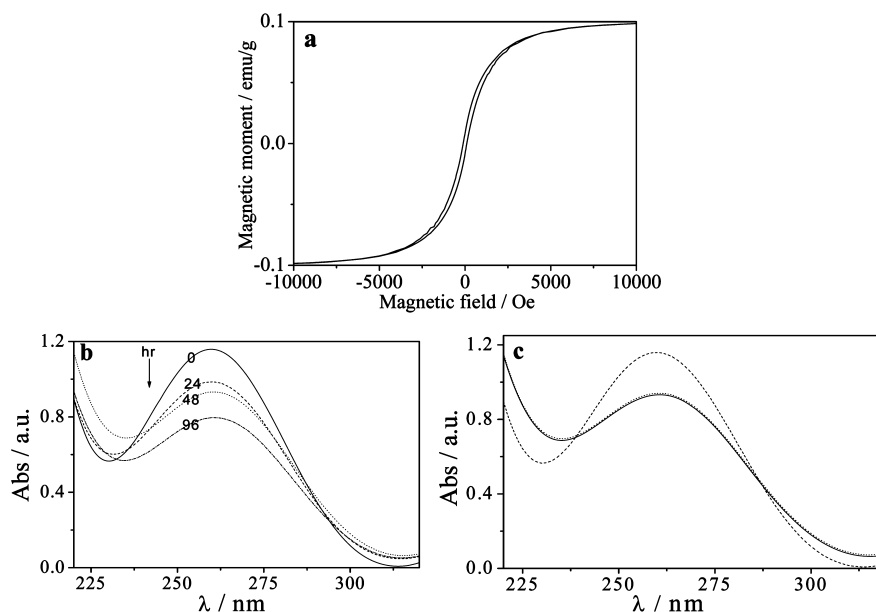

Figure 6. (a) SQUID magnetometry of the ferromagnetic DNA/azoTAFe complexes at 300 K. (b) UV evidence of the decrease in DNA concentration on the top of solution containing 0.075 mmol L^{-1} DNA and 0.01 mmol L^{-1} azoTAFe vs. time in the presence of an external magnetic field (0.25 T). (c) UV spectra of 0.075 mmol L^{-1} DNA/0.01 mmol L^{-1} azoTAFe complexes, the solid line refers to the sample after the introduction of a magnet for 48 h and the dotted one of the same sample after the magnet was removed for 48 h, the dashed line indicates the spectrum of stretched and uncompacted DNA.
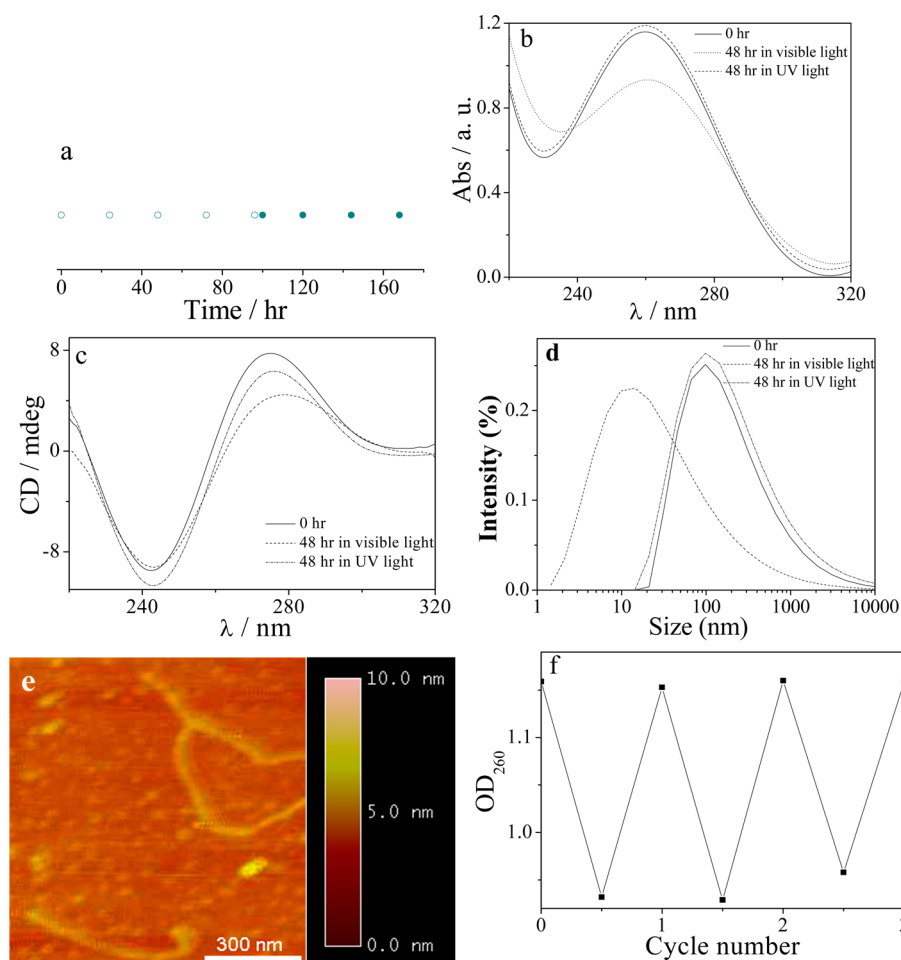
Figure 7. (a) Phase diagram, showing the time range where the compacted DNA placed in a magnetic field can be decompacted after UV irradiation. The open circles refer to the time range where compacted DNA can be recovered to original stretched coil state after UV irradiation, and the filled circles refers to those cannot be decompacted after being exposed to UV light. Evidences of the recovery of DNA to original coil state after UV irradiation detected by (b) UV spectra, (c) CD spectra, (d) DLS data. The recovery of DNA peaks in the three measurements indicates the appearance of the decompaction behavior. (e) AFM image of the DNA in Figure 4c decompacted to stretched state caused by the UV−vis irradiation. (f) Variation in OD_{260} with the conversion of light sources by means of using a magnet to induce the capture of DNA and using light to release DNA. $T = 25.0 \pm 0.1$ °C.

magnetic $[FeCl_3Br]^-$ ions in the Stern layer and those in the core of a cationic micelle.

The ability of azoTAFe in magnetizing DNA was used to control a magnetic field-based migration of DNA. As shown in the UV spectra (Figure 6b), in an applied magnetic field (0.25 T), apart from an efficient DNA compaction, with DNA magnetized by the surfactants, the resulting DNA/azoTAFe mixtures exhibit targeted migration toward the magnet surface. This behavior can improve the local concentration of DNA/azoTAFe complexes in the vicinity of magnetic fields, which finally made the complexes exceed the solubility limit and resulted in precipitates at the point of highest magnetic field density (Figure 3a). It was found that only 68.7% of the DNA remained in the upper solution 4 days later, others formed precipitates adjacent to the surface of the magnet (Figure 3a). This efficient migration of DNA/azoTAFe complexes toward an external magnetic field promises a bright future in targeted gene transfection. After removing the magnet, the magnetic induced DNA compaction can be stopped. The UV spectra of the sample of DNA/azoTAFe mixtures remain unchanged over time (Figure 6c), showing that further compaction, migration, and recovery of stretched DNA did not occur. This finding

shows that the magnetic switch can regulate the "on" and "off" of the DNA condensation and migration, but cannot independently reverse the compaction.

To realize the controllable capture and release of DNA, the magnetic switch needs to be reversible for higher compaction efficiency, a lower dosage, and potentials in targeted transport. As previously demonstrated, UV irradiation is effective in causing the release of DNA by triggering the trans-to-cis isotherm of azoTAFe which can disrupt the structure of micelles. We expected that the irreversibility of the magnetic switch can be complemented with UV irradiation. UV irradiation experiments on the samples of 0.075 mmol L^{-1} DNA and 0.01 mmol L^{-1} azoTAFe with different migration time in a magnetic field were conducted. The resulting phase diagram is presented in Figure 7a, which shows that the magnetic-induced DNA compaction can fully be recovered by UV illumination if the migration time of DNA/surfactant mixtures in a magnetic field was controlled within 96 h. The typical sample that gained an optimal compaction efficiency of 80% with a migration time at about 48 h was chosen to be determined by UV, CD, DLS, AGE measurements, and AFM observations. Total indications including recoveries in OD_{260}

Scheme 2. Schematic Diagram of the Dual-Switchable Capture and Release of DNA Regulated with Light Sources and a Weak Magnetic Field
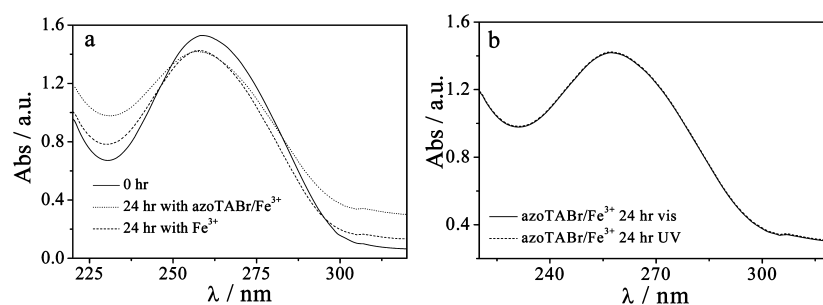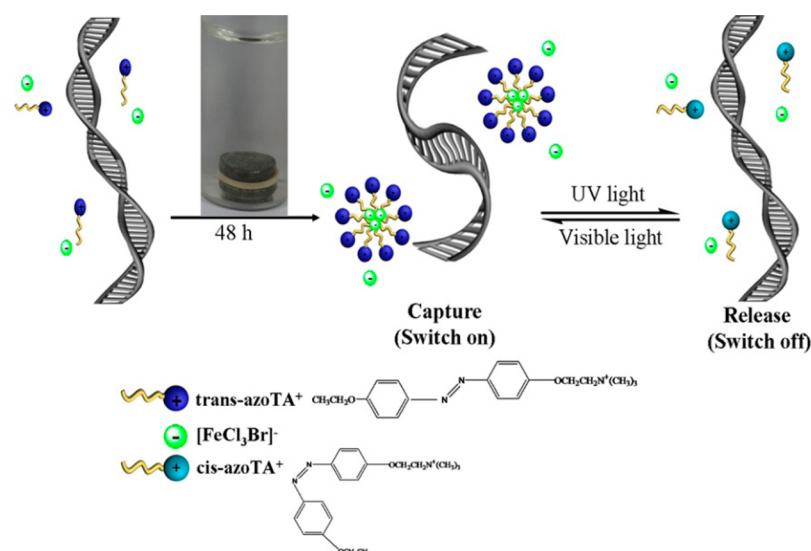

Figure 8. (a) UV evidence of the decrease in DNA on the top of solution vs. time induced by azoTABr/Fe^{3+} complex or Fe^{3+}. (b) UV evidence of the irreversibility of the azoTABr/Fe^{3+} complex induced magnetic field-based capture and migration of DNA after UV irradiation. $T = 25.0 \pm 0.1$ °C.

(Figure 7b), two main bands in CD spectra (Figure 7c), the size distribution in DLS data (Figure 7d), the fluorescent signal in AGE (lane 7 from Figure 3e), as well as the reappearance of DNA coils in AFM images (Figure 7e) indicate that the irreversibility of a magnetic field-induced DNA compaction and capture can be solved by means of UV irradiation, if the migration time of DNA can be controlled within 96 h. Variations in OD_{260} from about 0.940 in compacted state to about 1.155 in decompacted state with conversion of the light source (Figure 7f) show that this strategy in the manner of using a magnet to trigger the capture of DNA and then utilizing UV irradiation to release DNA is able to attain good reproducibility and stability.

    On the basis of all the results, the optimum strategy for using the dual-switches is below: (i) a magnetic field is applied to induce the capture of DNA with a lower dosage of azoTAFe, < cac, for 48 h. DNA can be compacted to reach the best efficiency; (ii) the reversible capture and release of DNA can be repeatedly regulated through converting light sources from UV to visible. A schematic diagram of this method is shown in Scheme 2.

    It is worth noting that, almost recently, Degen et al. reported that mixtures of cationic surfactant/Fe^{3+} show the same ability in magnetic control over liquid surface as that of the paramagnetic cationic surfactants with $[FeCl_3Br]^-$.[30] According to their opinion, there is no necessary to undergo an additional step to coordinate the $FeCl_3$ with Br^-. The property of

surfactant/Fe^{3+} mixtures in control over liquid surface can be explained by the interplay between the paramagnetic $FeCl_3$ solution and the reduction of surface tension by the surfactants.[30] On the basis of this, in our current work, we also conducted corresponding experiments to check out whether the mixtures of azoTABr/Fe^{3+} can result in the same property in control over the capture and release of DNA as the azoTAFe does. Corresponding experiments started with a magnet (0.25 T) placed at the bottom of a complex solution of 0.075 mmol L^{-1} DNA and 0.01 mmol L^{-1} azoTABr/Fe^{3+} (molar ratio = 1:1). After 24 h, an evident reduction of OD_{260} of DNA can be discovered (Figure 8a), suggesting that the mixtures of azoTABr/Fe^{3+} could exactly give out same ability in magnetic control over DNA migration as the azoTAFe does. However, this behavior could be reproduced by simply adding Fe^{3+} (Figure 8a), the resulting OD_{260} after 24 h is almost the same as that of azoTABr/Fe^{3+} complex. It seems that the migration of DNA is mainly regulated by Fe^{3+} and the presence of azoTABr did not result in much difference in controlling DNA. Referring to Bloomfield's work,[21] multivalent Fe^{3+} can exactly compact and capture DNA independently and the paramagnetism of Fe^{3+} guarantees that it can control a magnetic field-based migration of DNA. Degen and co-workers[30] ascribed the importance of using surfactants as the interfacial tension between the dodecane and water prevents the iron chloride transferring through the organic phase. In our case, it certainly does not need any reduction in the interfacial

tension as all compounds are placed in aqueous solution. Fe^{3+} can independently manipulate the compaction and migration of DNA in the absence of azoTABr. Furthermore, by virtue of the binding of Fe^{3+} cannot be reversed by UV illumination, one can easily understand that using azoTABr/Fe^{3+} complexes to control the capture and migration of DNA will be irreversible after exposing to the UV light. It was based on the fact that Fe^{3+} ions play a key role in controlling the DNA compaction and migration. Figure 8b confirms the irreversibility of the azoTABr/Fe^{3+}/DNA complex after UV illumination, because of no recovery of the OD_{260} being found. In the current system, the additional step of coordinating the Br^- with $FeCl_3$ should be undergone, in order to eliminate the interference of Fe^{3+} in compacting DNA and ensure that azoTAFe can not only provide an efficient magnetic field-induced capture and migration of DNA but also make the compacted and migrated DNA be effectively released after UV irradiation.

4. CONCLUSIONS

In conclusion, we designed and synthesized a novel dual-responsive cationic surfactant, azoTAFe, which contains both a light-responsive azobenzene group as well as a paramagnetic counterion, $[FeCl_3Br]^-$. This surfactant could abundantly utilize inexhaustible, clean sources, i.e., light and a magnetic field to act as two powerful switches for effectively controlling the capture and release of DNA. As proved, the light-responsive property leads to the variation in the cac of azoTAFe, which enables a reversible capture and compaction of DNA. On the basis of the paramagnetism of $[FeCl_3Br]^-$, an introduction of external magnetic field can clearly assist in enhancing the compaction efficiency from a maximum of 69−80% and can compact DNA with a lower dosage of delivery agent azoTAFe. In addition, the efficient migration of the ferromagnetic DNA/surfactant aggregates toward an external magnetic field shows potentials in achieving the targeted DNA transport. The light switch can solve the irreversibility of the magnetic-triggered DNA compaction and delivery with a short illumination time of only 5 min. The perfect self-complementation of the dual-responsive property in the functionality makes the azoTAFe an intelligent and versatile machine for regulating DNA trans-fection and gene delivery. We envisioned our results could find potential applications in gene therapy and biotechnology.

■ ASSOCIATED CONTENT

Ⓢ Supporting Information

Synthesis of the dual-responsive azoTAFe. SQUID magneto-metry and electrical conductivity results of azoTAFe. This material is available free in the charge via the Internet at http://pubs.acs.org/.

■ AUTHOR INFORMATION

Corresponding Author
*E-mail: shuli@sdu.edu.cn. Tel.: +86-531-88363768. Fax: +86-531-88564750.
Notes
The authors declare no competing financial interest.

■ ACKNOWLEDGMENTS

■ REFERENCES

(1) Eliyahu, H.; Servel, N.; Domb, A.; Barenholz, Y. Lipoplex-Induced Hemagglutination: Potential Involvement in Intravenous Gene Delivery. *Gene Ther.* **2002**, *9*, 850−858.

(2) Ulrich, A. S. Biophysical Aspects of Using Liposomes as Delivery Vehicle. *Biosci. Rep.* **2002**, *22*, 129−150.

(3) Szebeni, J.; Baranyi, L.; Savay, S.; Milosevits, J.; Bunger, R.; Laverman, P.; Metselaar, J.; Storm, G.; Chanan-Khan, A.; Liebes, L.; Muggia, F. M.; Cohen, R.; Barenholz, Y. Role of Complement Activation in Hypersensitivity Reactions to Doxil and Hynic PEG Liposomes: Experimental and Clinical Studies. *J. Liposome Res.* **2002**, *12*, 165−172.

(4) Wingard, J. R.; Leather, H. L.; Wood, C. A.; Gerth, W. C.; Lupinacci, R. J.; Berger, M. L.; Mansley, E. C. Pharmacoeconomic Analysis of Caspofungin versus Liposomal Amphotericin B as Empirical Antifungal Therapy for Neutropenic Fever. *Am. J. Health-Syst. Pharm.* **2007**, *64*, 637−643.

(5) Zuckermann, M. J.; Heimburg, T. Insertion and Pore Formation Driven by Adsorption of Proteins onto Lipid Bilayer Membrane-Water Interfaces. *Biophys. J.* **2001**, *81*, 2458−2472.

(6) Heimburg, T.; Marsh, D. Protein Surface-Distribution and Protein-Protein Interactions in the Binding of Peripheral Proteins to Charged Lipid Membranes. *Biophys. J.* **1995**, *68*, 536−546.

(7) Mel'nikov, S. M.; Sergeyev, V. G.; Yoshikawa, K. Discrete Coil-Globule Transistion of Large DNA Induced by Cationic Surfactant. *J. Am. Chem. Soc.* **1995**, *117*, 2401−2408.

(8) Mel'nikov, S. Y.; Lindman, B. pH-Controlled DNA Condensation in the Presence of Dodecyldimethylamine Oxide. *Langmuir* **2000**, *16*, 5871−5878.

(9) Dias, R. S.; Dawson, K.; Miguel, M. G. *DNA Interactions with Polymers and Surfactants*; Dias, R. S., Lindman, B., Eds.; John Wiley & Sons: New York, 2008; pp 89−111.

(10) Taylor, D. J. F.; Thomas, R. K.; Penfold, J. Polymer/Surfactant Interactions at the Air/Water Interface. *Adv. Colloid Interface Sci.* **2007**, *132*, 69−110.

(11) Carlstedt, J.; Lundberg, D.; Dias, R. S.; Lindman, B. Condensation and Decondensation of DNA by Cationic Surfactant, Spermine, or Cationic Surfactant-Cyclodextrin Mixtures: Macroscopic Phase Behavior, Aggregate Properties, and Dissolution Mechanisms. *Langmuir* **2012**, *28*, 7976−7989.

(12) Dias, R. S.; Lindman, B.; Miguel, M. G. Compaction and Decompaction of DNA in the Presence of Catanionic Amphiphile Mixtures. *J. Phys. Chem. B* **2002**, *106*, 12608−12612.

(13) Gonzalez-Perze, A.; Dias, R. S.; Nylander, T.; Lindman, B. Cyclodextrin-Surfactant Mixtures: A New Route in DNA Decom-paction. *Biomacromolecules* **2008**, *9*, 772−775.

(14) Dias, R. S.; Innerlohinger, J.; Glatter, O.; Miguel, M. G.; Lindman, B. Coil-Globule Transition of DNA Molecules Induced by Cationic Surfactants: A Dynamic Light Scattering Study. *J. Phys. Chem. B* **2005**, *109*, 10458−10463.

(15) Le Ny, A-L. M.; Lee, C. T. Photoreversible DNA Condensation Using Light-Responsive Surfactants. *J. Am. Chem. Soc.* **2006**, *128*, 6400−6408.

(16) Nalluri, S. K. M.; Voskuhl, J.; Bultema, J. B.; Boekema, E. J.; Ravoo, B. J. Light-Responsive Capture and Release of DNA in A Ternary Supermolecular Complex. *Angew. Chem., Int. Ed.* **2011**, *50*, 9747−9751.

(17) Brown, P.; Bushmelev, A.; Butts, C. P.; Cheng, J.; Eastoe, J.; Grillo, I.; Heenan, R. K.; Schmidt, A. M. Magnetic Control over Liquid Surface Properties with Responsive Surfactants. *Angew. Chem., Int. Ed.* **2012**, *51*, 2414−2416.

(18) Brown, P.; Bushmelev, A.; Butts, C. P.; Eloi, J. C.; Grillo, I.; Baker, P. J.; Schmidt, A. M.; Eastoe, J. Properties of New Magnetic Surfactants. *Langmuir* **2013**, *29*, 3246−3251.

(19) Gao, J.; Gu, H.; Xu, B. Multifunctional Magnetic Nanoparticles: Design, Synthesis, and Biomedical Applications. *Acc. Chem. Res.* **2009**, *42*, 1097−1107.

(20) Gu, H.; Xu, K.; Yang, Z.; Chang, C.; Xu, B. Synthesis and Celluar Uptake of Porphyrin Decorated Iron Oxide Nanoparticles-A

Potential Candidate for Biomodal Anticancer Therapy. *Chem. Commun.* **2005**, 4270−4272.

(21) Bloomfield, V. A. DNA Condensation by Multivalent Cations. *Biopolymers* **1997**, *44*, 269−282.

(22) Bionincontro, A.; Marchetti, S.; Onori, G.; Santucci, A. Complex Formation between DNA and Dodecyl-dimethyl-amine-oxide Induced by pH. *Chem. Phys. Lett.* **2003**, *370*, 387−392.

(23) Bionincontro, A.; La Mesa, C.; Proietti, C.; Risuleo, G. A Biophysical Invesitigation on the Binding and Controlled DNA Release in a Cetyltrimethyamounium Bromide-Sodium Octylsulfate Cat-anionic Vesicle System. *Biomacromolecules* **2007**, *8*, 1824−1829.

(24) Xu, L.; Chen, J.; Feng, L.; Dong, S.; Hao, J. Loading Capacity and Interaction Behaivor of DNA Binding on Catanionic Vesicles with Different Cationic Surfactants. *Soft Matter* **2014**, *10*, 9143−9152.

(25) Dobson, J. Gene Therapy Progress and Prospects: Magnetic Nanoparticles-based Gene Delivery. *Gene Ther.* **2006**, *13*, 283−287.

(26) Wiersma, P. H.; Loeb, A. L.; Overbeek, J. T. G. Calculation of the Electrophoretic Mobility of a Spherical Colloid Particle. *J. Colloid Interface Sci.* **1966**, *22*, 78−99.

(27) O'Brien, R. W.; White, L. R. Electrophoretic Mobility of A Spherical Collodial Particle. *J. Chem. Soc., Faraday Trans. 2* **1978**, *74*, 1607−1626.

(28) Bonincontro, A.; Falivene, M.; La Mesa, C.; Risuleo, G.; Pena, M. R. Dynamics of DNA Adsorption on and Release from SDS-DDAB Cat-anionic Vesicles: A Multitechnique Study. *Langmuir* **2008**, *4*, 1973−1978.

(29) Xu, L.; Feng, L.; Dong, R.; Hao, J.; Dong, S. Transfection Efficiency of DNA Enhanced by Association with Salt-free Catanionic Vesicles. *Biomacromolecules* **2013**, *14*, 2781−2789.

(30) Degen, P.; Zwar, E.; Paulus, M.; Tolan, M.; Pehage, H. About the Role of Surfactants on the Magnetic Control over Liquid Interfaces. *Langmuir* **2014**, *30*, 11563−11566.